Journal of Materials Chemistry C

Accepted Manuscript

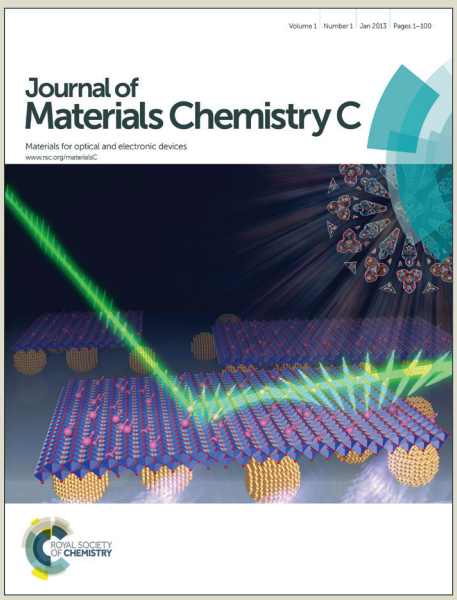

ROYAL SOCIETY OF CHEMISTRY

www.rsc.org/materialsC

Cite this: DOI: 10.1039/c0xx00000x

www.rsc.org/xxxxxx

ARTICLE TYPE

A Novel Luminescent Monolayer Thin Film based on Postsynthetic Method and Functional Linker

Ye Lu and Bing Yan*

Received (in XXX, XXX) Xth XXXXXXXXX 20XX, Accepted Xth XXXXXXXXX 20XX

DOI: 10.1039/b000000x

Abstract: Herein we report on a new strategy for fabricating luminescent monolayer thin film by modified metal-organic frameworks (MOFs). Lanthanide ion (Eu^{3+}, Tb^{3+} and Yb^{3+}) is introduced to MOFs (MOF-253) firstly, and then the second ligand TTA or TAA (TTA= 2-thenoyltrifluoroacetone and TAA= 1,1,1-trifluoropentane-2,4-dione) is used to further sensitize the lanthanide ion. Finally, the MOFs modified by lanthanide complex are assembled on quartz plate by functional linker. As-prepared MOF thin film is a dense and transparent monolayer, its thickness is less than 100 nm. Four kinds of optical functionalized MOF thin film are prepared by this method.

Introduction

Lanthanide complex-based porous materials have been achieved considerable attention as an important part of lanthanide organic-inorganic hybrids materials.[1] Up to now, lanthanide complex could be incorporated into various porous matrices, such as zeolites, MCM-41, MCM-48, and SBA-15(16) either by a simple doping method or by the covalent bond grafting technique.[2] For the stable structure and controllable size, a lot of research has focused on the application of zeolites incorporated lanthanide complex in optical materials.[3] Recently, this area is further promoted for the work reported by Li and coworker, about achieving higher organization and additional functionality by using a functional linker.[4] But the optical material based on zeolites also have some inherent flaw, for example, the less optical property of zeolites framework and the weaker effect (charge balance) between host and guest.[5]

Similarly with zeolites, metal-organic frameworks (MOFs) or porous coordination polymers (PCPs), a class of hybrid materials formed by the self-assembly of polydentate bridging ligands and metal-connecting points, are another famous crystalline porous material for structural diversity and outstanding tunability.[6] MOFs have the greater potential in the optical material. Because both the inorganic and the organic moieties can provide the platforms to generate luminescence, while metal-ligand charge and energy transfer related luminescence within MOFs also could add another dimensional luminescent functionalities.[7] Postsynthetic method (PSM), whose chemical modification can be performed on the fabricated material rather than on the molecule precursors, is another distinguished approach to imparting more sophisticated chemical and physical properties to MOF.[8] Actually, PSM for MOFs is similar to the so-called "ship in a bottle method", which is widely utilized in zeolite-based luminescent lanthanide materials.[9] MOFs used as a host matrix to carry lanthanide complex has just attracted the attention until recently: near-infrared light-emitting materials demonstrated by Carlos and coworker is designed by post-synthetic covalent modification of IRMOF-3 amino group followed by the coordination of Nd^{3+}/Y^{3+}.[10]

In the recent years, material processing based on MOFs is also an increasingly developing fields.[11] Especially, the processing of MOFs as films is a domain that has only recently been initiated but which is crucial role for many applications, such as chemical sensors and membranes.[12] In MOFs thin film, two class could be could be distinguished, polycrystalline films and SURMOFs.[13] The thickness of polycrystalline films is related to the size of the MOF particles or crystallites and often lies in the micrometer range, while the thicknees of SURMOFs is geneally more thin than former (in the nanometer range).[13a, 14] Actually, the inspiration of the fabrication of MOF thin films often comes from two closely related fields: zeolite films, particularly for polycrystalline films, and coordination polymer films.[15] For the reported MOFs thin films, almost of MOFs is directly connected to the matix rather than by some linker.[13a, 15] So this intrigues our interest in using the successful method on monolayer zeolite thin film (using functional linker) to achieve nanometer range monolayer polycrystalline MOFs thin film.

Here, we present a new strategy for preparing MOF-based monolayer luminescent thin film (Figure 1). Lanthanide complex (Eu^{3+}, Tb^{3+} and Yb^{3+}) is introduced to the MOF by PSM firstly, and then the MOFs modified by PSM could be assembled on quartz through functional linkers that has the ability to coordinate and sensitize lanthanide ion (Eu^{3+}, Tb^{3+} and Yb^{3+}). As-prepared MOF thin film is a dense and transparent monolayer with a high degree of coverage. Under the different excitation wavelength, the thin film could emit white, red, green light and near-infrared luminescence.

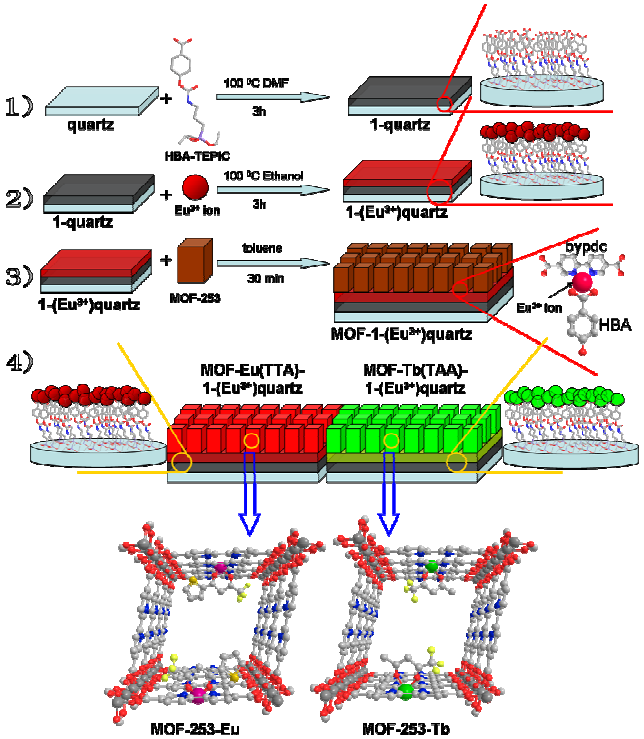

Figure 1 The procedure to prepare the thin film materials based on PSM and functional linker: (1) 1-quartz, (2) 1-(Eu^{3+})quartz, (3) MOF-1(Eu^{3+})quartz and (4) MOF-Eu(TTA)-1(Eu^{3+})quartz and MOF-Tb(TAA)-1(Tb^{3+})quartz.

Results and discussion

Preparation of MOF-253-Ln (Ln = Eu, Tb or Yb)

MOF-253 with a bipyridine derivative in the ligand, reported by Yaghi and co-workers, is famous in the inherent advantage of postsynthetic method (PSM). [8, 16] With PSM, the application of modified MOF-253 has been extended to catalysis and luminescent material.[17] In the structure of MOF-253, a one-dimensional infinite chains of AlO_6 corner-sharing octahedral is built by connecting bpydc (bpydc = 2,2'-bipyridine-5,5'-dicarboxylic) linkers to construct rhombic shaped pores. The representative structure of MOF-253 has been isolated by PXRD and a Pawley refinement using the Al(OH)(bpdc) ($bpdc^{2-}$ = 4,4-biphenyldicarboxylate) unit cell parameters in the reported work.[18] As-synthesized MOF-253 is confirmed by PXRD (Figure S1), elemental analysis (see experiment details), nitrogen adsorption/desorption isotherms (Figure S2) and FT-IR spectroscopy (Figure S3). The surface area of as-synthesized MOF-253 was considerably lower than Yaghi's work, but is consistent with other work about MOF-253.[16,17a] The corresponding transmission electron microscopy (TEM) image is shown in Figure S4, MOF-253 is a rectangle, whose length and width is about 100 and 30 nm, respectively.

MOF-253-Ln is prepared through PSM, in which lanthanide ions (Eu^{3+}, Tb^{3+} or Yb^{3+}) are firstly encapsulated to fabricated MOFs (MOF-253) host by coordination effect between Ln^{3+} ion and bipyridine of ligand, and then the second lignd TTA or TAA (TTA = 2-thenoyltrifluoroacetone and TAA 1,1,1-trifluoropentane-2,4-dione) is introduced to sensitizing incorporated Ln^{3+} ion. The as-synthesized MOF-253-Ln is confirmed by PXRD (Figure S1), elemental analysis (see experiment details), nitrogen adsorption/desorption isotherms (Figure S2) and FT-IR spectroscopy (Figure S3), respectively. After introducing Ln^{3+} ion and complex to MOF-253, the crystallization degree of MOF-253-based hybrid material is weakened, but the framework is not ruined (Figure S1). And then, the FT-IR spectroscopy can prove the integrity of framework, too. Bands at 1600 and 1420 cm^{-1} are observed in the FT-IR spectra of MOF-253 and MOF-253-Ln (Ln= Eu, Tb and Yb) which can be ascribed to the absorption of carboxylic group and bipyridine, respectively. The TEM of MOF-253-Eu also proves that the framework is intact because there is not obviously change in the morphology after PSM (Figure S5).

The excitation of MOF-253 is obtained by monitoring the emission at 550 nm, which is dominated by a broad band centered at about 370-390 nm in the near ultraviolet region (Figure S6). Under excitation at wavelengths of 380 nm, the emission spectra of pristine MOF-253 present broad bands centered at about 525-625 nm (Figure S6). The UV-visible diffuse reflectance spectrum (DRS) of MOF-253 is shown in the Figure S7. Actually, for the system with only one luminescent center, the UV-visible absorption spectrum is the same to the excitation. For the system with several luminescent centers, several luminescent centers would have several excitations, while the UV-Vis absorption spectrum is only one. So, for the system with several luminescent centers in the hybrid systems, the UV-Vis absorption spectrum is not consistent with every excitation spectrum and hence is a combination of all excitation spectra. For the MOF-253-based hybrid materials, the matrix MOF-253 is also a luminescent center and dominant. So the increase of absorbance in some direction is due to MOF-253. In the UV-visible diffuse reflectance spectrum for the solid samples of the hybrids, the negative peaks are due to the principle of DRS and Eu^{3+} emission. (Figure S7). The negative peaks are mean to the emission peaks. The data of DRS is record through integrating sphere, which can make the incident light to diffuse reflect. So, the incident light is not to reach the sample on the same time. The light which is early to reach the sample coan make the sample to emit light, but the intensity of the light is very weak, so only the Eu^{3+} ion which has stronger emission could get the emission on the DRS. The phenomenon is normally.

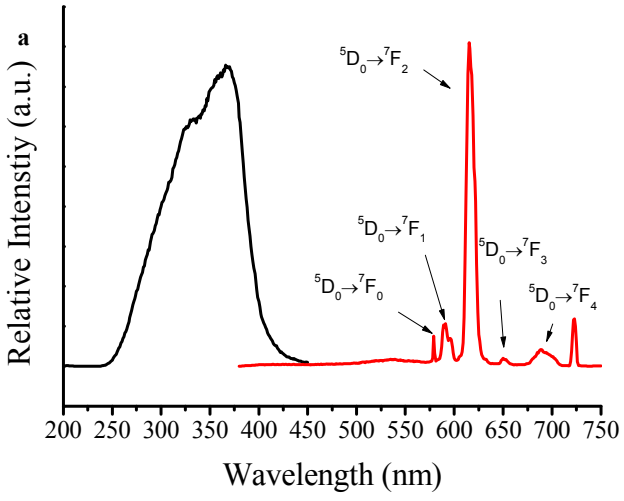

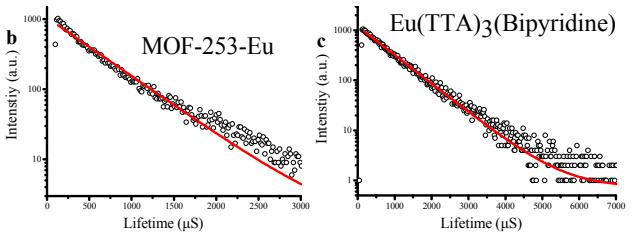

Figure 2 (a) The luminescent spectra of MOF-253-Eu (λ_{em} = 614 nm and λ_{ex} = 370 nm); decay curve of MOF-253-Eu (b) and Eu(TTA)$_3$(bipyridine) (c).

The emission of MOF-253-Eu exhibit the characteristic transitions of the Eu^{3+} ion at 579, 591, 614, 650 and 692 nm under the excitation of 370 nm, which are ascribed to the $^5D_0 \rightarrow {}^7F_0$, $^5D_0 \rightarrow {}^7F_1$, $^5D_0 \rightarrow {}^7F_2$, $^5D_0 \rightarrow {}^7F_3$ and $^5D_0 \rightarrow {}^7F_4$ transitions, respectively (Figure 2a). The excitation spectrum of MOF-253-Eu is obtained by monitoring the characteristic Eu^{3+} ion emission at 614 nm, which is dominated by a broad band centered at about 370 nm. The lifetime of MOF-253-Eu is 520 μs (Figure 2b). And the quantum yield (QY) is 11.3 % under the excitation at 370 nm.

Under excitation of 380 nm, the characteristic Eu^{3+} ion emission of MOF-253-Eu could be achieved too (Figure S8a). In comparison with the emission of MOF-253 with Eu^{3+} ion (without TTA) under 380 nm, the characteristic Eu^{3+} ion emission of MOF-253-Eu is obviously stronger than the former (Figure S8b). That proves the TTA coordinate with Eu^{3+} ion and efficiently sensitize to Eu^{3+} ion.

The complex Eu(TTA)$_3$(bipyridine) is prepared for further studying the effect between host and guest, and Eu(TTA)$_3$(bipyridine) is checked by elemental analysis (see experiment details), DRS (Figure S7) and luminescent spectra (Figure S9). The lifetime of Eu(TTA)$_3$(bipyridine) (758 μs) is longer than the complex introduced to MOF (Figure 2c). That means there is energy transfer from framework to the Eu^{3+} ion.

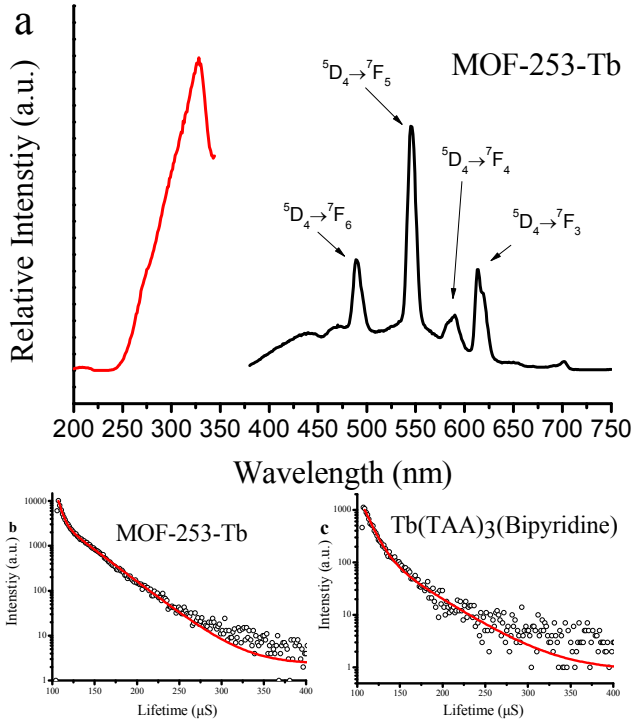

Figure 3 (a) The luminescent spectra of MOF-253-Tb (λ_{em} = 545 nm and λ_{ex} = 330 nm); and the decay curve of MOF-253-Tb (b) and Tb(TAA)$_3$(bipyridine) (c).

Similar situation occurs in MOF-253-Tb. It is hard to achieve the characteristic Tb^{3+} ion emission for MOF-253 with Tb^{3+} ion (without TAA) because of the overlap of emission of MOF-253 and Tb^{3+} ion. After introducing TAA, the characteristic Tb^{3+} ion emission could be observed in the MOF-253-Tb (Figure 3a). The emission line of MOF-253-Tb was assigned to the $^5D_0 \rightarrow {}^7F_J$ (J = 6, 5, 4 and 3) transitions at 491, 545, 588 and 613 nm, respectively. The MOFs' strangest emission peak (at 550 nm) overlaps with the Tb^{3+} ion characteristic emission (Figure S10). So, in excitation spectra, the band about 380 nm from framework is obviously stronger than the Tb^{3+} ion excitation band (Figure 3a and S10). The excitation spectra of MOF-253-Tb was obtained by monitoring the emission of Tb^{3+} ions at 545 nm and is dominated by a shoulder band centered at 330 nm which is the characteristic absorption of the lanthanide complexes arising from the energy transition based on the second ligand, TAA. The lifetime of MOF-253-Eu is 16 μs (Figure 3b). And the quantum yield (QY) is 9.3 % under the excitation at 330 nm.

The lifetime of Tb(TAA)$_3$(bipyridine) (26 μs) is longer than MOF-253-Tb (Figure 3c). The Tb(TTA)$_3$(bipyridine) is checked by elemental analysis (see experiment details), DRS (Figure S7) and luminescent spectra (Figure S11). In view of emission of MOF overlapped with Tb^{3+} ion, the decrease of the measured Tb^{3+} lifetime of MOF-253-Tb relatively to the Tb(TAA)$_3$(bipyridine) may be due to the contribution of the MOF-253 emission or to the presence of non-radiative sites.

The emission intensity of MOF-253-Yb is very low because the excitation light source is Xe lamp. So, the characteristic emission of Yb^{3+} ion can not be detected for MOF-253 with Yb^{3+} ion (without TAA). After introducing TAA, though the intensity of emission is still not satisfactory, the $^2F_{5/2} \rightarrow {}^2F_{7/2}$ transition of Yb^{3+} could be identified (Figure S12). The sensitization of β-diketones to lanthanide ion has been studied for a long time.[1, 19] The sensitization of TAA to Yb^{3+} ion could be explained by schematic energy level diagrams (Figure S13). The energy is transferred from TAA to $^2F_{5/2}$, and then to $^2F_{7/2}$.[20]

Preparation of MOF-1(Eu^{3+})-quartz thin film

The flexible linker 1, HBA-TEPIC (HBA = 1, 4-hydroxybenzoic acid, TEPIC = 3- (triethoxysilyl)-propyl-isocynate) has a urea groups, a triethoxysilyl group and a carboxyl group (Figure S14a).[21] As is show in the Figure 1, the urea is used for the formation of H-bonding between the linker, the triethoxysilyl is used for binding to the OH groups on the quartz plate and the carboxyl group could react with Ln^{3+} ion to achieve 1(Ln^{3+})-quartz (step 2). The HBA-TEPIC is checked by ^{1}H NMR (see experiment details) and UV-visible absorbance spectrum (Figure S14b).

One simple and direct method of checking the presence of linker 1 on the quartz plates is to contact the 1-quartz plate with a solution of Eu^{3+} ion in ethanol to prepared the 1-(Eu^{3+})quartz. After immersed in solution of Eu^{3+} ion in ethanol, the quartz plates display red light upon irradiation under UV. Figure S15 shows the luminescent spectra of 1-(Eu^{3+})quartz, the excitation was obtained by monitoring the $^5D_0 \rightarrow {}^7F_2$ of Eu^{3+} ions at 616 nm. The broad band with maximum at 330 nm in the excitation

spectrum can be ascribed to Eu-O charge transfer that could be used to sensitize Eu^{3+} ion. The five prominent emission lines peaking at 588, 592, 616, 651 and 698 nm in the emission spectrum can be assigned to the $^5D_0 \rightarrow {}^7F_J$ (J = 0-4) transition with red emission for J = 2 as the dominant feature. This proves that the HBA moiety on the substrate absorbs energy and transfers to the Eu^{3+} ion. Vigorous stirring of the substrate in ethanol cannot cause any decrease in the emission intensities of Eu^{3+}, suggesting that Eu^{3+} is coordinated to the HBA and tethered on the substrate.

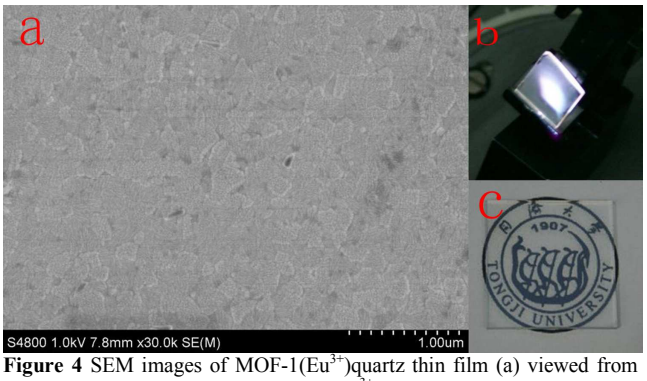

Figure 4 SEM images of MOF-1(Eu^{3+})quartz thin film (a) viewed from surface, the white light from MOF-1(Eu^{3+})quartz under the light of 390 nm (b) and the photograph of MOF-1(Eu^{3+})quartz thin film (c).

The functionalized plates, 1(Eu^{3+})-quartz, could be further immersed in a suspension of MOF-253 in toluene to realize step 3, the formation of MOF-1(Eu^{3+})-quartz (Figure 1). Here, Eu^{3+} ion is used as linker to connect the MOF-253 and the functionalized plates.

The transparent Eu-HBA-functionalized quartz plates (1(Eu^{3+})-quartz) turn opaque upon contact with the suspension of MOF-253 in dry toluene under vigorous sonication as described in the experimental section. The opaque samples become transparent after sonication for approximately 5 s in pure toluene to remove physisorbed excess of nanoparticle. The scanning electron microscopy (SEM) images of the modified quartz plates (MOF-1(Eu^{3+})-quartz) reveal that the coverage degree and packing degree are both highly satisfactory although some spots with less surface coverage can be observed in Figure 4a. And then, the thin film is transparent in the photograph (Figure 4c). SEM images of MOF-1(Eu^{3+})quartz thin film viewed from cross-section is shown in Figure S16. The thickness of the thin film should be less than 100 nm in that there are some particles of MOF-253 whose size is less than 100 nm. The Energy Dispersive Spectroscopy (EDS) further prove the thin film is MOF-253 (Figure S17).

The luminescent spectra of MOF-1(Eu^{3+})-quartz (λ_{em} = 616 nm and λ_{ex} = 326 nm) are shown in Figure 5a. The emission spectra of these MOF-253-based quartz plate exhibit the characteristic transitions of the Eu^{3+} ion at 573, 590, 616, 649 and 698 nm, which are ascribed to the $^5D_0 \rightarrow {}^7F_0$, $^5D_0 \rightarrow {}^7F_1$, $^5D_0 \rightarrow {}^7F_2$, $^5D_0 \rightarrow {}^7F_3$ and $^5D_0 \rightarrow {}^7F_4$ transitions, respectively. In comparison with the emission of 1-(Eu^{3+})quartz, the intensity at 450-550 is obviously stronger than the above. This is due to the luminescence of framework. The excitation spectra were obtained by monitoring the $^5D_0 \rightarrow {}^7F_2$ of Eu^{3+} ions at 616 nm.

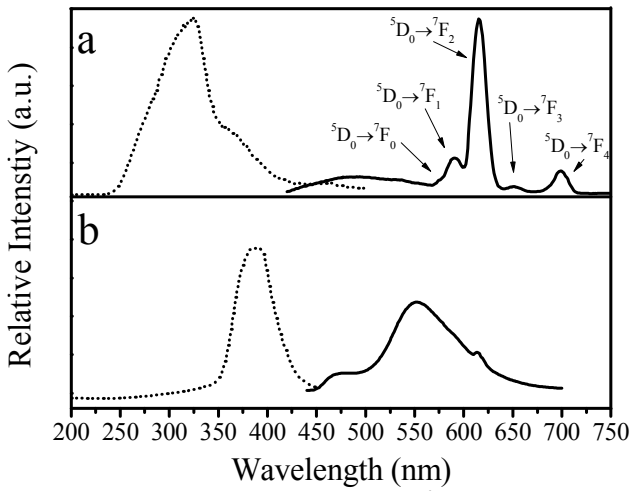

Figure 5 The luminescent spectra of MOF-1-(Eu^{3+})quartz: (a) (λ_{em} = 616 nm and λ_{ex} = 328 nm); (b) (λ_{em} = 550 nm and λ_{ex} = 380 nm).

When the MOF is used as luminescent center, the excitation of MOF-1-(Eu^{3+})quartz is obtained by monitoring the emission at 550 nm, which is dominated by a broad band centered at about 370-390 nm in the near ultraviolet region (Figure 5b). Under excitation at wavelengths of 380 nm, the emission of MOF-1-(Eu^{3+})quartz present broad bands centered at about 525-625 nm. The luminescent spectra are similar to the primitive MOF-253 (Figure S6), expect for some subtle different in the emission spectra for the existence of Eu^{3+} ion. This proves the MOF-253 has been successfully connected on the Eu-HBA-functionalized quartz plate. The point of emission spectrum of MOF-1(Eu^{3+})-quartz under 390 nm in CIE chromaticity diagram is in the area of yellow color (Figure S18). So the white light could be archived by the yellow light (from MOF) and the violet light (from the excited light). The CIE points of phosphor and points of excitation light (round the color area) could construct a line (Figure S18). And every point of this line could be achieved by different contents of phosphors. This is similar to the principle of current white LEDs for solid-state lighting which are based on blue InGaN substrate that excites a yellow-emitting YAG: Ce phosphor. A cold white light could be achieved by the combination of blue (from substrate) and yellow light (from phosphor).[22] For MOF-1(Eu^{3+})-quartz, the CIE points is X=0.36 and Y= 0.50. The line of CIE point and 390nm (round the color area) is cross the white light. That means the white light could be achieved by MOF-1(Eu^{3+})-quartz under 390 nm. In the photograph of MOF-1(Eu^{3+})quartz, the thin film could emit white light under 390nm (Figure 4b).

According to Judd-Ofelt theory, the $^5D_0 \rightarrow {}^7F_1$ transition of Eu^{3+} is of magnetic-dipole nature and insensitive to site symmetry, while $^5D_0 \rightarrow {}^7F_2$ is of electric-dipole nature and very sensitive to site symmetry. So, the intensity ratio of $^5D_0 \rightarrow {}^7F_2$ to $^5D_0 \rightarrow {}^7F_1$ is usually used to investigate the symmetry of Eu^{3+} ion.[23] The intensity ratio of $^5D_0 \rightarrow {}^7F_2$ to $^5D_0 \rightarrow {}^7F_1$ changes from 7.1 for 1(Eu^{3+})-quartz to 11.3 for MOF-1(Eu^{3+})-quartz. This also demonstrates the coordination effect reaction of Eu^{3+} ion with bipyridine. For the further proving the vital role of Eu^{3+} ion in linking MOF-253 and quartz, we have added a contrast experiment which is with and without Eu^{3+} ion. An excess of MOF-253 was added to toluene and sonicated for approximately

30 min, the 1-quartz were introduced , and the mixture was then sonicated for 15 min, like the process of synthesis MOF-1(Eu^{3+})-quartz. But the white light like MOF-1(Eu^{3+})-quartz is not observed in the quartz without Eu^{3+} ion after mixing with MOF-253. That is anther solid evidence to prove the Eu^{3+} ion as a bridge of linking MOF-253 and quartz.

Preparation of MOF-Ln(TTA/TAA)-1(Ln^{3+})-quartz (Ln = Eu, Tb or Yb)

MOF-Ln(TTA/TAA)-1(Ln^{3+})-quartz (Ln=Eu^{3+}, Tb^{3+} or Yb^{3+}) is prepared by the similar way of MOF-1(Ln^{3+})-quartz with replacing the MOF-253 as MOF-253-Ln (Ln=Eu^{3+}, Tb^{3+} or Yb^{3+}). Meanwhile, 1(Eu^{3+})-quartz is replaced by 1(Tb^{3+})-quartz and 1(Yb^{3+})-quartz. The emission of these MOF-Eu(TTA)-1(Eu^{3+})-quartz, as similar with MOF-253-Eu, exhibit the characteristic transitions of the Eu^{3+} ion at 577, 592, 612, 651 and 693 nm under the excitation of 368 nm, which are ascribed to the $^5D_0\rightarrow{}^7F_0$, $^5D_0\rightarrow{}^7F_1$, $^5D_0\rightarrow{}^7F_2$, $^5D_0\rightarrow{}^7F_3$ and $^5D_0\rightarrow{}^7F_4$ transitions, respectively (Figure 6a). Compared with 1(Eu^{3+})-quartz, the excitation of MOF-Eu(TTA)-1(Eu^{3+})-quartz occurs obviously red shift, the peak changes from 330 nm (1(Eu^{3+})-quartz) to 368 nm (MOF-Eu(TTA)-1(Eu^{3+})-quartz). This is attributed to the sensitization of TTA to the Eu^{3+} ion. The TTA absorb energy in the UV area and then transfer to the Eu^{3+} ion. In the photograph, the MOF-Eu(TTA)-1(Eu^{3+})-quartz emits bright red light under 368 nm. The luminescent spectra of MOF-Eu(TTA)-1(Eu^{3+})-quartz is similar to the MOF-253-Eu. This is due to the intensity of MOF-Eu(TTA)-1(Eu^{3+})-quartz is obviously larger than the 1(Eu^{3+})-quartz (Figure S19).

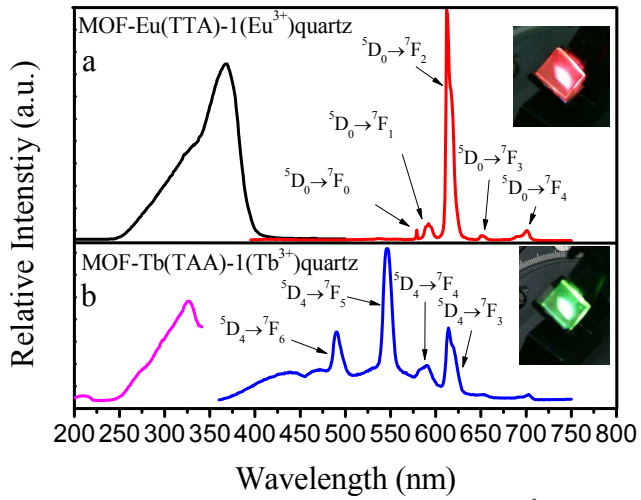

Figure 6 The luminescent spectra of MOF-Eu(TTA)-1-(Eu^{3+})quartz (a) (λ_{em} = 612 nm and λ_{ex} = 368 nm) and MOF-Tb(TAA)-1-(Tb^{3+})quartz (b) (the λ_{em} = 545 nm and the λ_{ex} = 326 nm), the photograph of MOF-Eu-1-(Eu^{3+})quartz is taken under 368 nm, the photograph of MOF-Tb-1-(Tb^{3+})quartz is taken under 326 nm

The same situation also occurs to MOF-Tb(TAA)-1(Tb^{3+})-quartz and MOF-Yb(TAA)-1(Yb^{3+})-quartz. The luminescent spectra of MOF-Tb(TAA)-1(Tb^{3+})-quartz and MOF-Yb(TAA)-1(Yb^{3+})-quartz are similar to the MOF-253-Tb and MOF-253-Yb. The excitation of MOF-Tb(TAA)-1(Tb^{3+})-quartz was obtained by monitoring the emission of Tb^{3+} ions at 545 nm and is dominated by a shoulder band centered at 326 nm (Figure 6b and S20). The emission line of the hybrid materials was assigned to the $^5D_0\rightarrow{}^7F_J$ (J = 6, 5, 4 and 3) transitions at 491 nm, 545 nm, 588 nm and 613 nm, respectively (Figure 6b). The luminescent spectra of MOF-Yb(TAA)-1(Yb^{3+})-quartz are displayed in Figure S21. There is a broad excitation from 350–400 nm. The emission displays the typical Yb^{3+} emission at approximately 984 nm under 380 nm, corresponding to the $^2F_{5/2}\rightarrow{}^2F_{7/2}$ transition of Yb^{3+}.

The lifetime of MOF-Eu(TTA)-1(Eu^{3+})-quartz is 499 μS (Figure S22), which is also close to the MOF-253-Eu. It is worth to notice that the lifetime of MOF-based thin film is shorter than the zeolite L modified by Eu^{3+} ion TTA, and phen (620 μs).[5a] This may be due to the energy transfer from framework to Eu^{3+} ion. The lifetime of MOF-Tb(TAA)-1(Tb^{3+})-quartz is 15 μs (Figure S23). The absolute quantum yield of MOF-Eu-1(Eu^{3+})-quartz and MOF-Tb(TAA)-1(Tb^{3+})-quartz is determined to be 11.4 % and 9.7 %, respectively, under the excitation at 368 nm for Eu^{3+} ion and 326 nm for Tb^{3+} ion.

Conclusions

In summary, a new strategy of designing visible and NIR monolayer thin film based on PSM and functional linker has been proposed. As-prepared MOF thin film is a dense and transparent monolayer with a high degree of coverage. Under the different excitation wavelength, the thin film could emit visible and near-infrared luminescence according to different lanthanide ion. Furthermore, this method also can be conveniently applied to other MOF-based thin film materials, whose desired properties can be tailored by an appropriate choice of linker, MOF and lanthanide complex.

Experimental

Chemicals

Chemicals were purchased from commercial sources. All solvents were analytical grade and without further purification. Linker 1 was synthesized and characterized according to the procedure reported in reference.[S1] Quartz plates (10 × 10 mm) were dipped into an acid bath consisting of potassium dichromate and sulfuric acid for 12 hrs to remove possible organic residues on the surface. The plates were then washed with copious amounts of deionized water and dried at 80 °C in Ar for 3 hrs. $Eu(NO_3)_3{\cdot}xH_2O$, $Tb(NO_3)_3{\cdot}xH_2O$ and $Yb(NO_3)_3{\cdot}xH_2O$ were prepared by dissolving oxides (Eu_2O_3, Tb_4O_7 or Yb_2O_3) in concentrated nitric acid (HNO_3). MOF-253 (Al(OH)(bpydc)) is synthesized according to the references.[S2]

Synthetic procedures

MOF-253. MOF-253 was prepared from hydrothermal reaction of $AlCl_3{\cdot}6H_2O$ (151 mg, 0.625 mmol), 2,2'-bipyridine-5,5'-dicarboxylic acid (153 mg, 0.625 mmol) and 10 mL N,N'-dimethylformamide (DMF) at 120 °C for 24 hrs. The resulting white microcrystalline powder was then collected with by centrifugation and washed with DMF. The solid products were washed with methanol viasoxhlet extraction for 24 hrs, and then was collected by filtration and finally dried at 200 °C under vacuum for 12 hrs to give [Al (bpydc)(OH)], MOF-253 (165 mg, 90 %). Anal. Calcd for $C_{12}H_7AlN_2O_5$: C, 50.34; H, 2.45; N, 9.79. Found: C, 50.29; H, 2.52; N, 9.74.

MOF-253-Ln (Ln = Eu, Tb and Yb). The preparation of MOF-253-Eu was carried out as follows: The compound

Al(OH)(bpydc) (47 mg, 0.15 mmol), solution of $Eu(NO_3)_3{\cdot}xH_2O$ in the acetonitrile (3.75 mL, 2 mmol/L) and acetonitrile (15 mL) were added to a Tefloncapped 20 mL scintillation vial and heated on a hotplate at 65 °C for 24 hrs. The resulting white solid product was collected by centrifugation and washes with acetonitrile by ultrasonic three times. The resulting product was collected by filtration and heated at 60 °C for 12 hrs under vacuum. The resulting product (47 mg, 0.15 mmol), solution of TTA in the acetonitrile (0.45 mL, 50 mmol/L), thriethylamine in the acetonitrile (0.45 mL, 50 mmol/L) and acetonitrile (15 mL) were added to a Tefloncapped 20 mL scintillation vial and heated on a hotplate at 65 °C for 24 hrs. The resulting white solid product was collected by centrifugation and washes with acetonitrile by ultrasonic three times and dried at 60 °C under vacuum for 12 hrs to give $[Al(bpydc)(OH)(Eu(NO_3)_3)_{0.05}(TTA)_{0.15}]$, MOF-253-Eu (42 mg, 89 %). Anal. Calcd. for $C_{12.24}H_{7.09}AlEu_{0.01}N_2O_{5.06}S_{0.03}F_{0.09}$: C, 49.95; H, 2.42; N, 9.52. Found: C, 49.97; H, 2.45; N, 9.39. MOF-253-Tb and MOF-253-Yb was prepared in a similar manner to MOF-253-Eu, but the ligand is replaced as TAA. (Generally, one trivalent lanthanide ion could coordinate with three β-diketone molecules. So, the ratio of TTA and Eu is 3:1. And then, in the process of reaction, the feed ratio of TTA and Eu^{3+} ion is 3:1.)

$Eu(TTA)_3$(bipyridine). $Eu(NO_3)_3{\cdot}xH_2O$ (446 mg, 1 mmol), 2-thenoyltrifluoroacetone (TTA) (666 mg, 3 mmol) and triethylamine (303 mg, 3 mmol) was dissolved in 15 mL ethanol. The solution was yellow and clear. The bipyridyl (156 mg, 1 mmol) and H_2O was added and deposit appears immediately. The deposite was collected by filtration and cleaned by ethanol. After drying under vacuum, the product was white powder (802 mg). Yield is 87 %. Anal. Calcd. for $C_{34}H_{23}EuF_9N_2O_6S_3$: C, 41.90; H, 2.38; N, 2.87. Found: C, 41.54; H, 2.56; N, 2.58.

$Tb(TAA)_3$(bipyridine). $Tb(TAA)_3$(bipyridine) is prepared by the same ways of $Eu(TTA)_3$(bipyridine), but using Tb $(NO_3)_3{\cdot}xH_2O$ and TAA. Anal. Calcd. for $C_{25}H_{17}TbF_9N_2O_6$: C, 38.92; H, 2.22; N, 3.63. Found: C, 38.94; H, 2.26; N, 3.68.

Linker 1 (HBA-TEPIC). 2.0 mmol (0.497 g) of 3-(triethoxysilyl)-propyl-isocyanate (TEPIC) was added dropwise to an acetone solution, where 1,4-hydroxybenzoic acid (HBA) (2 mmol, 0.279 g) was dissolved with stirring under an argon atmosphere. The mixture was heated with reflux at 60 °C in a covered flask for approximately 13 hrs. The coating liquid was concentrated to remove the solvent acetone using a rotary vacuum evaporator and a yellow viscous liquid sample was obtained. And then the yellow liquid sample was dissolved in absolute ethanol, and 20 mL of hexane was added into the solution to precipitate. Subsequently, the solution was filtrated and white powder was obtained. The above procedures of dissolution and filtration were repeated three times. At last the pure white powder was obtained and dried in a vacuum. ($C_{16}H_{26}N_2O_7Si$) The ^{1}HNMR (DMSO-d6) data are as follows: 0.49 (2H, t), 1.09 (9H, t), 1.45 (2H, m), 2.93 (2H,t), 3.72 (6H, m), 3.96 (1H, t), 6.82 (2H, d), 7.78 (2H, d), 10.41 (1H, s).

1-quartz. Typically, the quartz plates were immersed in a solution of linker 1 (0.5 mmol) in dry DMF (10 mL) and heated at reflux for 3h under Ar, cooled to room temperature, and washed with copious amounts of DMF

1(Ln^{3+})-quartz (Ln = Eu, Tb and Yb). $Eu(NO_3)_3{\cdot}xH_2O$, $Tb(NO_3)_3{\cdot}xH_2O$ or $Yb(NO_3)_3{\cdot}xH_2O$ in ethanol (0.1 M, 2 mL) and equimolar triethylamine was added to 1-quartz in DMF(10 mL), and the mixture was stirred at 100 °C for 3 hrs. After cooling room temperature, the functionalized 1(Ln^{3+})-quartz samples were removed from the flask and wash with copious amounts of ethanol.

MOF-1(Eu^{3+})-quartz. An excess of MOF-253 (10 mg) was added to toluene (10 mL) and sonicated for approximately 30 min, the pretreated quartz plates (1(Eu^{3+})-quartz) were introduced , and the mixture was then sonicated for 30 min. The opaque quartz plates coated with MOF-253 were sonicated in toluene for 5 s to remove the physisorbed crystals.

MOF-Ln-1(Ln^{3+})-quartz (Ln = Eu, Tb and Yb). MOF-Ln-1(Ln^{3+})-quartz (Ln = Eu, Tb or Yb) is prepared by the same way of MOF-1(Eu^{3+})-quartz, but the MOF-253-Eu is replaced by MOF-253-Tb and MOF-253-Yb, and then, 1(Eu^{3+})-quartz is replaced by 1(Tb^{3+})-quartz and 1(Yb^{3+})-quartz.

Physical characterization

The elemental analyses of nitrogen and carbon element the hybrids are measured with a Vario ELIII elemental analyzer. X-ray diffraction patterns (SAXRD) are recorded on a Rigaku D/max-Rb diffractometer equipped with a Cu anode in a 2θ range from 5 to 45 °. Scanning electronic microscope (SEM) was measured on Hitachi S-4800. Transmission electron microscope (TEM) experiments were conducted on a JEOL2011 microscope operated at 200 kV or on a JEM-4000EX microscope operated at 400 kV. Nitrogen adsorption/desorption isotherms are measured by using a Nova 1000 analyzer under the liquid nitrogen temperature. Luminescence excitation and emission spectra of the solid samples are obtained on Edinburgh FLS920 spectrophotometer. Luminescence lifetime measurements are carried out on an Edinburgh FLS920 phosphorimeter using a microsecond pulse lamp as excitation source. The data of life time is achieved from fitting the experiment luminescent decay. The measurement of quantum yield (QY) is made by exciting the samples with diffuse light within an integrating sphere.

Notes and references

Department of Chemistry, Tongji University, Shanghai 200092, P. R. China. Fax: (+86) 21-65982287; E-mail: byan@tongji.edu.cn

† Electronic Supplementary Information (ESI) available: See DOI: 10.1039/b000000x/

1 (*a*) K. Binnemans, *Chem. Rev.*, 2009, **109**, 4283; (*b*) L. Rozes and C. Sanchez, *Chem. Soc. Rev.*, 2011, **40**, 1006; (*c*) L. D. Carlos, R. A. Ferreira, V. de Zea Bermudez, B. Julian-Lopez and P. Escribano, *Chem. Soc. Rev.*, 2011, **40**, 536.

2 (*a*) J. Feng and H. J. Zhang, *Chem. Soc. Rev.*, 2013, **42**, 387; (*b*) L. D. Carlos, R. A. Ferreira, Z. Bermudez Vde and S. J. Ribeiro, *Adv. Mater.* 2009, **21**, 509; (*c*) B. Yan, *Rsc Adv.*, 2012, **2**, 9304; (*d*) G. Calzaferri, S. Huber, H. Maas and C. Minkowski, *Angew. Chem. Int. Edit.*, 2003, **42**, 3732; (*e*) S. N. Huber and G. Calzaferri, *Angew. Chem. Int. Edit.*, 2004, **43**, 6738; (*f*) Y. Li and B. Yan, *Micropor. Mesopor. Mater.*, 2010, **128**, 62; (*g*) Y. J. Gu and B. Yan, *Eur. J. Inorg. Chem.*, 2013, 2963; (*h*) Y. J. Li, B. Yan and L. Wang, *Dalton Trans.*, 2011, **40**, 6722.

3 (*a*) G. Calzaferri, S. Huber, H. Maas and C. Minkowski, *Angew. Chem. Int. Edit.*, 2003, **42**, 3732; (*b*) K. B. Yoon, *Accounts Chem. Res.*, 2007, **40**, 29.

4 (*a*) Y. Wang, H. R. Li, Y. Feng, H. J. Zhang, G. Calzaferri and T. Z. Ren, *Angew. Chem. Int. Edit.*, 2010, **49**, 1434; (*b*) P. P. Cao, Y. G. Wang, H. R. Li and X. Y. Yu, *J. Mater. Chem.*, 2011, **21**, 2709.

5 (*a*) Y. X. Ding, Y. G. Wang, H. R. Li, Z. Y. Duan, H. H. Zhang and Y. X. Zheng, *J. Mater. Chem.*, 2011, **21**, 14755; (*b*) H. R. Li, Y. X. Ding, P. P. Cao, H. H. Liu and Y. X. Zheng, *J. Mater. Chem.*, 2012, **22**, 4056.

6 H. C. Zhou, J. R. Long and O. M. Yaghi, *Chem. Rev.*, 2012, **112**, 67.

7 (*a*) Y. J. Cui, Y. F. Yue, G. D. Qian and B. L. Chen, *Chem. Rev.* 2012, **112**, 1126; (*b*) J. Rocha, L. D. Carlos, F. A. A. Paz and D. Ananias, *Chem. Soc. Rev.*, 2011, **40**, 926.

8 S. M. Cohen, *Chem. Rev.*, 2012, **112**, 970-1000.

9 A. Mech, A. Monguzzi, F. Meinardi, J. Mezyk, G. Macchi, R. Tubino, *J. Am. Chem. Soc.*, 2010, **132**, 4574-4575.

10 R. M. Abdelhameed, L. D. Carlos, A. M. S. Silva and J. Rocha, *Chem. Commun.*, 2013, **49**, 5019.

11 D. Farrusseng, *Metal-organic frameworks : applications from catalysis to gas storage*, Wiley-VCH, Weinheim, 2011.

12 (*a*) L. E. Kreno, K. Leong, O. K. Farha, M. Allendorf, R. P. Van Duyne and J. T. *Hupp, Chem. Rev.*, 2012, **112**, 1105; (b)J. Gascon, F. Kapteijn, *Angew. Chem. Int. Edit.*, 2010, **49**, 1530; (c) S. Sorribas, P. Gorgojo, C. Tellez, J. Coronas and A. G. Livingston, *J. Am. Chem. Soc.*, 2013, **135**, 15201; (*d*) G. Lu, O. K. Farha, L. E. Kreno, P. M. Schoenecker, K. S. Walton, R. P. Van Duyne and J. T. Hupp, *Adv. Mater.* 2011, **23**, 4449; (*e*) P. A. Szilagyi, R. J. Westerwaal, R. van de Krol, H. Geerlings and B. Dam, *J. Mater. Chem. C*, 2013, **1**, 8146.

13 (*a*) A. Betard and R. A. Fischer, *Chem. Rev.*, 2012, **112**, 1055; (b) M. C. So, S. Jin, H. J. Son, G. P. Wiederrecht, O. K. Farha and J. T. Hupp, *J. Am. Chem. Soc.*, 2013, **135**, 15698; (*c*) K. Otsubo, T. Haraguchi, O. Sakata, A. Fujiwara and H. Kitagawa, *J. Am. Chem. Soc.*, 2012, **134**, 9605.

14 (*a*) H. L. Guo, Y. Z. Zhu, S. L. Qiu, J. A. Lercher and H. J. Zhang, *Adv. Mater.*, 2010, **22**, 4190; (*b*) R. Makiura, S. Motoyama, Y. Umemura, H. Yamanaka, O. Sakata and H. Kitagawa, *Nat. Mater.*, 2010, **9**, 565.

15 (*a*) O. Shekhah, J. Liu, R. A. Fischer and C. Woll, *Chem. Soc. Rev.*, 2011, **40**, 1081; (*b*) D. Zacher, O. Shekhah, C. Woll and R. A. Fischer, *Chem. Soc. Rev.*, 2009, **38**, 1418.

16 E. D. Bloch, D. Britt, C. Lee, C. J. Doonan, F. J. Uribe-Romo, H. Furukawa, J. R. Long and O. M. Yaghi, *J. Am. Chem. Soc.*, 2010, **132**, 14382.

17 (*a*) F. Carson, S. Agrawal, M. Gustafsson, A. Bartoszewicz, F. Moraga, X. D. Zou and B. Martin-Matute, *Chem-Eur. J.*, 2012, **18**, 15337; (*b*) M. Wang, B. Z. Yuan, T. M. Ma, H. F. Jiang and Y. W. Li, *Rsc Adv.*, 2012, **2**, 5528; (*c*) Y. Y. Liu, R. Decadt, T. Bogaerts, K. Hemelsoet, A. M. Kaczmarek, D. Poelman, M. Waroquier, V. Van Speybroeck, R. Van Deun and P. Van Der Voort, *J. Phys. Chem. C*, 2013, **117**, 11302.

18 I. Senkovska, F. Hoffmann, M. Froba, J. Getzschmann, W. Bohlmann and S. Kaskel, *Micropor. Mesopor. Mater.*, 2009, **122**, 93.

19 S. B. Meshkova, Z. M. Topilova, D. V. Bolshoy, S. V. Beltyukova, M. P. Tsvirko and V. Y. Venchikov, *Acta. Phys. Pol. A*, 1999, **95**, 983.

20 (*a*) S. Singaravadivel, E. Babu, M. Velayudham, K. L. Lu and S. Rajagopal, *Polyhedron*, 2013, *60*, 54; (*b*) R. Pappalardo and D. L. Wood, *J. Chem. Phys.*, 1960, **33**, 1734.

21 X. F. Qiao and B. Yan, *Dalton Trans.*, 2009, 8509.

22 (*a*) C. Rhonda, *Luminescence: From Theory to Applications*, Wiley-VCH Verlag GmbH and Co: Weinheim, 2008; (*b*) G. Blasse, B. C. Grabmaier, *Luminescent Materials*, Springer-Verlag: New York, 1994.

23 M. P. Hehlen, M. G. Brik and K. W. Kramer, *J. Lumin.*, 2013, **136**, 221.